

Research Article · DOI: 10.2478/s13230-012-0007-2 · JBR · 2(4) · 2011 · 185-192

Investigating improvements to neural network based EMG to joint torque estimation

Mervin Chandrapal^{1*}, XiaoQi Chen¹, WenHui Wang¹, Benjamin Stanke², Nicolas Le Pape³

Mechatronics Research Laboratory,
Department of Mechanical Engineering,
University of Canterbury,
Christchurch, New Zealand

2 University of Applied Sciences, Factorial 5: Nature and Engineering, School of Biomimetics, Bremen, Germany

3 Ecole Nationale Supérieure d'Ingénieurs de Limoges, 16 rue Atlantis, Parc ESTER Technopole, Limoges, France

> Received 2011/10/26 Accepted 2012/01/09

Abstract

Although surface electromyography (sEMG) has a high correlation to muscle force, an accurate model that can estimate joint torque from sEMG is still elusive. Artificial neural networks (NN), renowned as universal approximators, have been employed to capture this complex nonlinear relation. This work focuses on investigating possible improvements to the NN methodology and algorithm that would consistently produce reliable sEMG-to-knee-joint torque mapping for any individual. This includes improvements in number of inputs, data normalization techniques, NN architecture and training algorithms. Data (sEMG) from five knee extensor and flexor muscle from one subject were recorded on 10 random days over a period of 3 weeks whilst subject performed both isometric and isokinetic movements. The results indicate that incorporating more muscles into the NN and normalizing the data at each isometric angle prior to NN training improves torque estimation. The mean lowest estimation error achieved for isometric motion was 10.461% (1.792), whereas the lowest estimation errors for isokinetic motion were larger than 20%.

Kevwords

EMG to Force · powered assistive device · artificial neural networks

1. Introduction

Muscles are both the dominant tissue and the primary organ of the human body. An estimated 70% to 85% of gross body weight is attributed to muscles [1]. Skeletal muscle, which is the type of muscle of interest here, produces torque across a joint by shortening its resting length. On a macroscopic level skeletal muscles are classified by their line of action, direction of pull and their origins and insertions 2. tional unit of the neuromuscular system is the motor unit (MU). MUs consist of an α -motor neuron and connected muscle fibres [2]. The α -motor neurons, located in the brain stem and spinal cord, create an electrical impulse (action potential) that travels along axons to its terminal branches, each of which is connected to a single muscle fibre at the neuromuscular junction. The connection is usually in the middle or proximal to the middle of the muscle fibre. As the action potential (AP) reaches the muscle fibres, depolarization of the fibre membrane triggers muscle contraction [3]. The membrane depolarization causes a time-varying transmembrane electric current field that can be measured non-invasively from the surface of the skin above the muscle

[4]. Since a single action potential will only cause a twitch, it is necessary for the motor neuron to generate a series of APs in order to achieve a longer period of contraction.

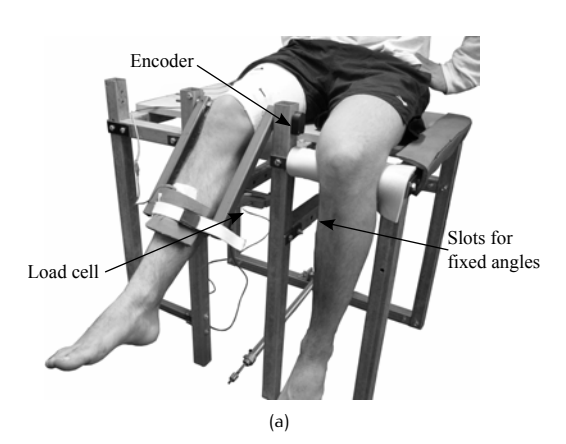
The Myoelectric Signal (MES) detected on the skin surface using surface Electromyography (sEMG) is the algebraic summation of these APs [5]. As these waves are bi-phasic or tri-phasic, the phase cancellation that consequently occurs, results in the detected sEMG having an amplitude less than proportional to the number of MU firing per second. The amplitude of the detected sEMG also varies significantly as a result of the summation [6]. Other factors that can vary from day to day (or session to session) and may affect the sEMG but not the internal MES, include blood flow, the condition of the skin surface and the position of the electrodes on the muscle [1]. Furthermore, sEMG can only be reliably measured from superficial skeletal muscles. Despite these limitations, sEMG have been shown to have a very high parallelism to muscular movement and force [7]. Thus extracting and modelling this sEMG-to-joint-torque relationship is especially useful in the field of powered prosthetics, actuated assistive/rehabilitative devices and for monitoring muscle recovery during rehabilitation [8].

Research into identifying the exact relation between sEMG and joint torque has been carried out for more than half a century, and many models have been proposed [2], the most common of which is the Hill model or a variation of it. The classical three-element Hill elastic muscle model approximates skeletal muscles' mechanical responses using passive and active elements, in parallel and series configuration. When considering a coordinated movement, the net force from all muscles involved can be summed to determine the resultant joint movement. This approach was recently employed for a knee exoskeleton developed by

^{*}E-mail: mervin.chandrapal@pg.canterbury.ac.nz

The point where the muscle attaches to the bone close to the centre of the body

² The point where the muscle attaches to the bone furthest from the centre of the body



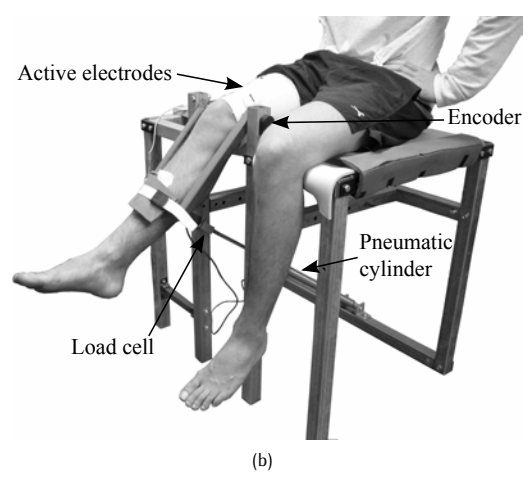


Figure 1. Isometric (a) and isokinetic (b) test rig setup

[9] in his thesis work. Calibration of all parameters necessary for the exoskeleton was substantial and experimental results obtained showed that there were limitations to the method. A disadvantage with this approach is that "assumptions have to be made at each step about largely unknown properties of the musculoskeletal and nervous system" [10] as the number of muscles modelled increases. Alternatively, the utilization of fast and efficient machine learning algorithms to map the nonlinear sEMG-to-joint-torque relation is an approach that has gained much interest in the past decade. In particular, the Multilayer Perceptron neural network (MLP) has gained popularity because of its capacity as a universal approximator [11]. These techniques are particularly useful when *exact* force from each muscle in the musculoskeletal system is not as important as the total resultant movement of the joint, such as in a control system for an actuated prosthetic or assistive device.

In [12] the authors implemented a three-layer MLP to derive an EMG-to-force relationship. EMG and joint force data were obtained *in vivo* from a load cell and electrodes that were implanted in adult cats. Although the method was invasive, the results obtained prove the suitability of the Neural Network (NN) to map the EMG to muscular force relationship. In

[10], a non-invasive approach to estimate isokinetic³ elbow-joint torque using a three-layer MLP was attempted. The mapping was carried out using data from 5 different subjects. Surface EMG from the biceps brachii and triceps brachii were assumed to be representative of the flexors and extensors of the elbow. The trained NN had a minimum estimation error of 0.0277 (RMSD) prompting the conclusion that the NN is an effective tool for this purpose. Hahn [13] extended the application of MLP for isokinetic joint torque estimation to the knee joint. In his work, data were collected from 20 subjects and sEMG from the vastus lateralis (VL) and biceps femoris (BF) were assumed to represent the attrication of knee extensors and flexors. He too concluded that the three-layer MLP is a feasible technique for estimating isokinetic joint torque

Based on results obtained in [13], we have further investigated the sEMG-to-joint-torque relation, with the specific goal of obtaining a feasible NN model for the knee joint, that can be utilized in a sEMG-based control system for an actuated assistive device. Thus the focus is not to obtain a general physiological model, but rather a specific mapping algorithm and method that would produce consistent joint torque mapping, with acceptable estimation errors, for any individual. There are still a few questions regarding the sEMG-to-joint-torque mapping that have not been explored. For example:

- Will the inclusion of more knee extensor and flexor muscles improve joint torque estimation? In the previous work only one knee extensor and one flexor muscle were used.
- Will alternative data normalization methods prior to NN training improve isometric⁴ torque estimation?
- Is there another more efficient NN architecture and training algorithm that could surpass the MLP in knee joint torque estimation?
- If a set of neurons in the NN produce the best solution on one day, will it also produce a near-optimal solution on another day with the same type of test, thus ensuring the robustness of the NN architecture over multiple sessions? Both previous papers [10, 13] have only tried to find optimal number of neurons in the MLP for different subjects rather than for the same subject over multiple days.
- Is it possible to estimate isokinetic torque using a NN trained with isometric data, by assuming quasi-static motion at low velocities?

In this work, we have attempted to provide answers to these questions through experimental results. This paper is organized as follows; in Section 2 the experimental setup, signal processing and data normalization techniques are discussed. The two NNs used in this work are described in Section 3. The experimental results obtained are shown and discussed in Section 4. The paper is concluded in Section 5.

 $^{^{3}}$ Motion where the velocity of the moving limb is controlled i.e. constant velocity, allowing maximal force to be exerted throughout the range of motion.

⁴ Muscular contraction against resistance without movement such that the length of the muscle does not change, i.e. constant joint angle



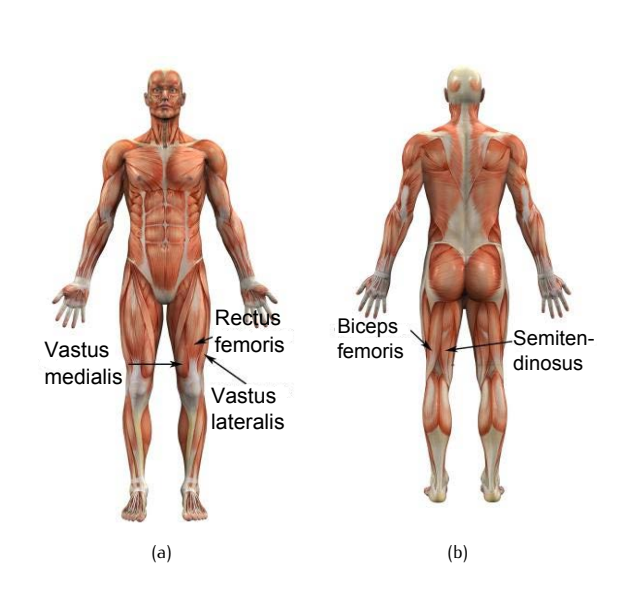
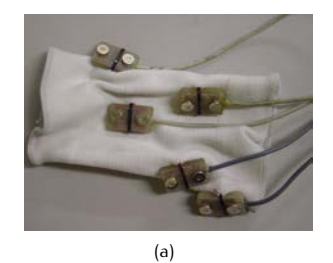


Figure 2. The quadriceps (vastus intermedius not shown) (a) and hamstring muscles (b) [14]

2. Experimental procedure

The experiments were carried out with one subject (physically healthy, 26-year-old male, weight: 66kg, height: 1.74m), on 10 random days, over a period of three weeks to incorporate inter- and intra-session variation. The test procedure was explained to the subject and written consent was obtained prior to participation. The test apparatus was constructed to allow the measurement of isometric torque at seven different angles (0°, 15°, 30°, 45°, 60°, 75°, 90°), and isokinetic torque at any given angular velocity (Fig. 1(a)). The subject was seated in a reclining position with his back supported and the rotation axis of his right knee along the sagittal plane was aligned to the rotation axis of the apparatus. The subject's leg was fastened to the moveable arm of the apparatus using straps at the distal end of the tibia. The neutral position was defined as the position when the knee joint was fully extended. At this position the encoder (US digital S5-360) mounted at the rotation axis of the apparatus was zeroed. The maximum angle was when the knee was flexed 90°, as measured through the encoder. The moveable arm of the apparatus could be rigidly fixed at any of the seven angles by means of a link that passed through a load cell. A PID-controlled pneumatic cylinder provided variable resistance for the isokinetic tests (Fig. 1(b)). On each of the 10 days, data from three sessions of seven isometric tests at the seven angles $(0^o, 15^o, 30^o, 45^o, 60^o, 75^o, 90^o)$, and four isokinetic tests at 5^os^{-1} , 10^os^{-1} , 15^os^{-1} , 20^os^{-1} were collected. The isokinetic speeds were chosen to include a slow to moderate walking pace, similar to the gait of people who require assistance. The subject was allowed a 2 minute break between each test and one hour between each session. For the isometric tests, the subject was instructed to exert maximum effort for knee extension followed by a maximum effort for knee flexion. Then at each isokinetic speed the subject was encouraged to exert maximum eccentric and concentric contraction throughout the range of motion (93° to -2°). Surface EMG from three knee extensor muscles and two knee flexors together with torque data were recorded. The muscles were chosen based on their percentage cross sectional area (%PCA) and



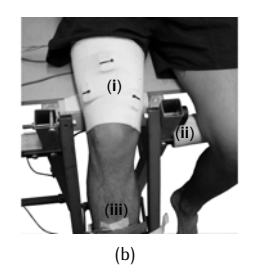


Figure 3. Bipolar active electrodes (a) and placement on leg (b). Where (i) Active electrodes, (ii) Encoder, and (iii) Ground electrode.

the ability of signal detection using surface electrodes. The extensor muscles are the vastus lateralis (VL;20%), rectus femoris (RF;8%) and vastus medialis (VM;15%). Although the vastus intermedius has a significant contribution to knee joint extension, sEMG from this muscle is difficult to detect as it is located beneath the RF. The flexor muscles are the semitendinosus (ST;3%), and biceps femoris (BF;10%) [15]. The location of the knee extensor and flexor muscles are shown in Fig. 2.

2.1. Electrodes

sEMG were recorded through five pairs of nickel-plated active bipolar surface electrodes shown in Fig. 3. The reusable electrodes were constructed with a built in pre-amplifier (4000x amplification) circuit. The dimension (circular electrodes, 10mm diameter in the direction of the muscle fibre) and the inter-electrode distance (20mm) was fixed based on SENIAM recommendations [16]. Prior to placement, the electrodes were gelled and the placement site was shaved and cleaned with alcohol to reduce surface impedance. During reattachment on subsequent days, care was taken (visually) to ensure that the electrodes were placed at the same site. The bipolar surface electrodes were placed proximal to the midpoint of each muscle belly, to avoid the innervation zones and to reduce cross talk [17]. Guidelines provided by Cram [1] were used as reference for electrode placement. The reference electrode was attached on the front of the tibia on the same leg (right leg).

2.2. Data processing

sEMG signals

All five pre-amplified sEMG signals are sampled simultaneously at 2kHz. Typically the sEMG signals are then band-pass filtered at approximately 20Hz to 500Hz [7, 13, 18]. Recent research however has shown that force information is contained in the higher frequency segment of the sEMG [2, 19]. Therefore in this work, all sEMG were bandpass filtered from 400-600Hz using a 2^{nd} order Butterworth filter. The signal was then rectified and low pass filtered (1.5Hz- 2^{nd} Order Butterworth filter) to obtain the activation envelope. The low pass filtering replicates the 2^{nd} order muscle twitch response to the impulse from the motor unit action potential [20]. The phase lag that results from this filtering also reproduces the electromechanical delay ($60 \rightarrow 120$ ms) in the cross bridge mechanism [20].

Torque and position data

Torque information was obtained through a load cell (PT AST 250) mounted on the link that secured the moveable arm of the apparatus. The load cell was sampled at 100Hz and synchronized with the sEMG

signals, then low pass filtered at 30Hz (2^{nd} Order Butterworth filter) to remove noise [19, 21]. Position and velocity data were sampled at 2kHz from the encoder mounted on the test rig.

2.3. Data normalization

The main purpose of data normalization is to provide a common basis of comparison across different sessions and different subjects. Luh [10] used the peak sEMG and torque value recorded during Maximum Voluntary isometric Contraction (MVC) for both flexion and extension at 90° (elbow angle) to normalize all data. Similarly, Hahn [13] also used the peak MVC data at a single angle (45° knee angle) to normalize all subsequent data. However, the effect of different methods of sEMG and torque data normalization on the NN prediction has not been thoroughly investigated. In this work, sEMG and torque data were normalized using two methods. The first used the same method employed in [13], i.e. normalization of all data with respect to the maximum values at 45° knee angle. The second method was to normalize the isometric sEMG and torque data from each of the seven angles with respect to its own maximum, at each angle. This was based on results obtained in [19, 22, 23] which propose that for isometric contractions the shape of the torque (force) vs. sEMG curve is similar for each angle once normalized. Muscle force-length relationship is well described in literature and [24] has shown that the normalized force-length curve is similar at different joint angles for in vivo human skeletal muscles. As there were three sessions conducted each day resulting in three isometric tests for each angle, the mean maximum sEMG and torque value at a given angle was used to normalize all data for that angle. The mean of the maximum values was used as it provided a robust estimate of the MVC at every angle. In the case of the first method, the mean maximum of all three tests at 45° was used for normalization.

The sEMG and torque normalizations are described by Equations 1 and 2 respectively. Where $nEMG_m$ is the normalized sEMG, $n\tau$ is the normalized torque and $sEMG_m^\alpha$ is the sEMG data of muscle m (VL, RF, VM, BF and ST) at knee angle α (0°, 15°, 30°, 45°, 60°, 75°, 90°). The mean maximum sEMG of muscle m at knee angle α is represented as $\mu_{\rm max}sEMG_m^\alpha$ and n is the number of sessions per day (i.e. 3), where i increases from 1 to 3. Similar notation also applies for torque normalization.

$$nEMG_{m,i}^{\alpha} = \frac{sEMG_{m,i}^{\alpha}}{\mu_{m\alpha x}sEMG_{m}^{\alpha}}$$
(1)
$$\mu_{max}sEMG_{m}^{\alpha} = \frac{\sum_{i}^{n} \max(sEMG_{m,i}^{\alpha})}{n}$$
$$n\tau_{i}^{\alpha} = \frac{\tau_{i}^{\alpha}}{\mu_{max}\tau^{\alpha}}$$
(2)
$$\mu_{max}\tau^{\alpha} = \frac{\sum_{i}^{n} \max(\tau_{i}^{\alpha})}{n}$$

Isokinetic data normalization

Isokinetic motion data were normalized to the same mean maximum values used to normalize isometric data for a given day. In the first method, all isokinetic data were normalized to the mean maximum isometric contraction values at 45^{o} knee angle. With the second method the isokinetic data were normalized with respect to mean maximum values at each of the seven isometric angles. For intermediate knee angles without actual values, linear interpolation was used to approximate the mean maximums.

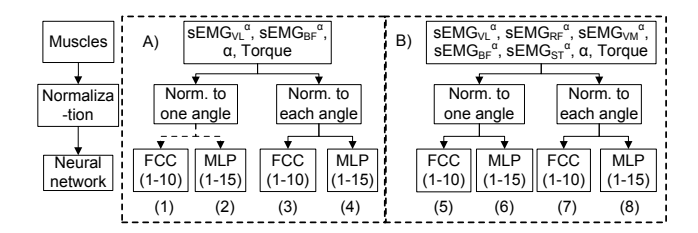


Figure 4. Flowchart of isometric data normalization and NN training

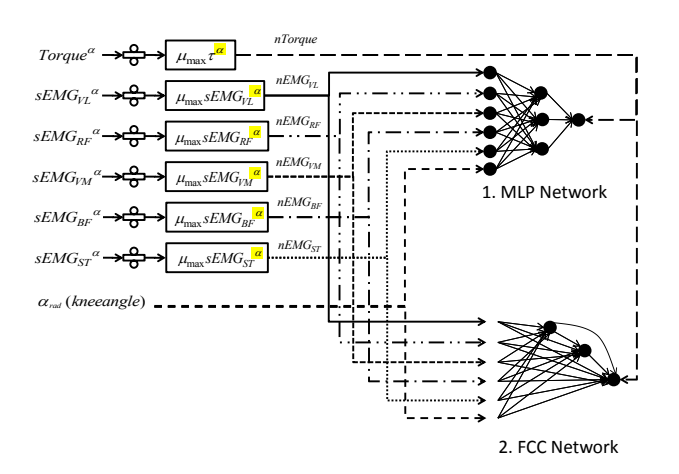
Methods

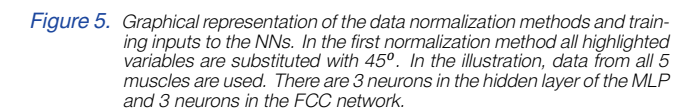
Neural networks, initially inspired by biological information processing, have proven to be excellent non-linear function approximators. The Multilayer Perceptron (MLP) architecture with three layers (input \rightarrow hidden \rightarrow output) is the most common NN implemented. A good overview of its general architecture and mathematical representation can be found in [11]. Based on the architecture and training algorithm used in [10, 13] a three-layer MLP network, trained using the second-order-gradient-based Levenberg-Marquardt (LM) algorithm, was also implemented in this work. Training of the network was halted when either the gradient was sufficiently small (less than 1e-5), the number of epochs exceeded 1000 or the generalization error (used as an early stopping criterion) started to increase indicating that overfitting had occurred. The training of the NN was then repeated with an increased number of neurons (1 \rightarrow 15) in the hidden layer.

In addition to the standard MLP NN, the recently developed Neuronby-Neuron (NBN) algorithm, claimed to have significant improvements over the well known LM algorithm, was also implemented. Among the advantages of the NBN over the LM are its ability to handle arbitrarily connected NN which should result in smaller networks, requiring only the forward computation without the backpropagation process, and also the ability to directly compute the quasi-Hessian matrix; both of which should reduce the computation time [25]. Furthermore, Wilamowski [25-28] proposed that the standard MLP is not the most efficient neural network available. Using parity problems he demonstrated that the Fully Connected Cascade (FCC) network is more powerful than the classical MLP algorithm. In our work, this FCC network trained using the NBN algorithm was implemented alongside the MLP (trained with the LM algorithm) to provide an experimental comparison for this particular application. The FCC network was also repeatedly trained with an increasing number of neurons in the network (1 \rightarrow 10) to determine the optimum network size. To the authors' knowledge, this is the first time the NBN algorithm has been utilized to model the sEMG-to-joint-torque relationship.

The training of the NN using data acquired on each of the 10 days is illustrated in Fig. 4. The procedure in block A is essentially repeated in block B, with the difference that more muscles were used for the joint torque estimation. In block A, data from only two muscles (VL-extensor and BF-Flexor) along with the joint angle α , were used to estimate the joint torque whereas in block B data from all five muscles were utilized to train the NN. The next level down on Fig. 4 shows the normalization methods. Each set of data was normalized using method one or method two as discussed in Section 2.3. At the lowest level, the normalized data were used to train the two NNs. The data from the first two sessions in a day were randomly partitioned; 60% used to train the NN, 20% used for testing and 20% used for validation and early stopping. Then the network was tested with data from the third session. This







gives an unbiased indication of the NNs generalization. There were 8 test categories each day with increasing NN size resulting in a total of 100 NN trained for each day. For each of the 8 categories, the NN size that has the lowest average estimation error was chosen as the best result. The NN estimation error was measured as a percentage root mean squared difference (%RMSD) and is described in Equation 3, where \hat{y} is the estimated normalized torque and y is the actual normalized torque [19]. Only the estimation errors from the *third session* were used to calculate the average estimation error. The best 8 NNs were then utilized to estimate isometric torque for the other 9 days, to test the ability of the NN to identify day to day sEMG to torque relationship, without new learning. Finally, the best networks were tested with the normalized isokinetic data to determine NN's ability to estimate dynamic torque. Fig. 5 gives a graphical representation of the data normalization methods and the NN training architectures.

$$%RMSD = RMS(y - \hat{y})/RMS(y) \times 100$$
 (3)

4. Results and discussion

The experiments were carried out over a period of three weeks to incorporate natural variations that occur in sEMG and joint torque. Since the main purpose of this study is to identify possible improvements that will enable a NN to give accurate and repeatable estimate of knee joint torque from sEMG for a given person, incorporating as much variation as possible in the relationship is a necessary condition. The maximum isometric knee extensor and flexor torques over the 10 days were found to be quite consistent. The mean (\bar{x}) and standard deviation (σ) of the maximum torque is shown in Fig. 6. Comparatively, flexor torques have a smaller σ than extensor torques. With regards to sEMG data, large variations were recorded over the same 10 day period. Fig. 7 shows the plot of the normalized mean maximum sEMG. The σ (not shown in figure) ranged from as small as 0.097 to as large as 0.971. One consistent result was that the peak extensor and flexor torques which

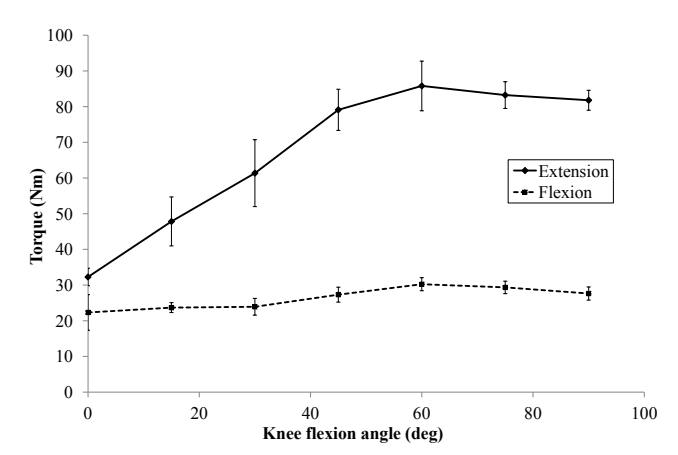


Figure 6. Mean maximum isometric knee extensor and flexor torque over 10 days

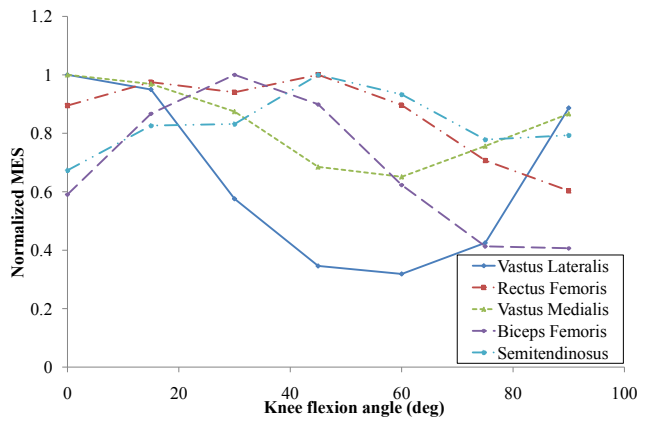


Figure 7. Normalized mean maximum sEMG from all five muscles

occurs at $60^{\it o}$ never coincided with the peak sEMG from any of the five muscles.

It was also observed that joint torque estimation errors were larger at smaller knee flexion angles especially at 0^{o} , which always had the highest %RMSD. Conversely, the lowest %RMSD was usually at 45^{o} or 60^{o} knee flexion. The high %RMSD at smaller angles may be attributed to the effect of passive forces across the knee joint. It is well known that passive forces across a joint increase near the limits of its motion. Since these forces are not reflected in the measured sEMG, the NNs are unable to fully capture their effects. However, incorporating the joint angle as an input to the NN improves the torque estimation [10].

4.1. Number of Muscles

The influence of incorporating multiple flexor and extensor muscles on joint-torque estimation was investigated using the two procedures shown in Fig. 4. The mean lowest estimation errors for both procedures over the three-week period are plotted in Fig. 8. Joint-torque estimation using data from five muscles results in an improvement of

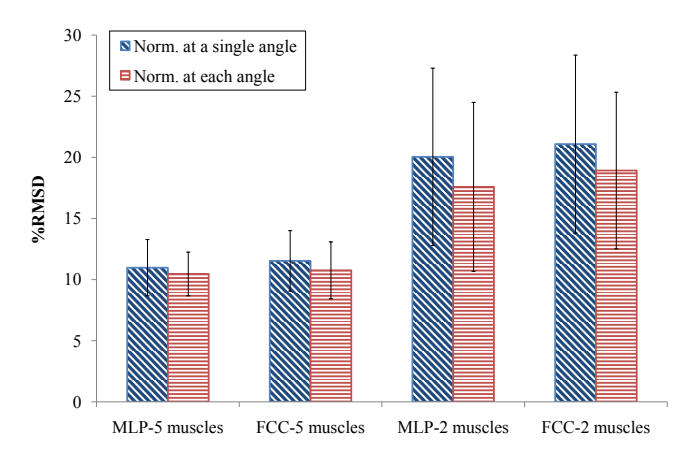


Figure 8. Mean lowest %RMSD for each normalization method and NN algorithm

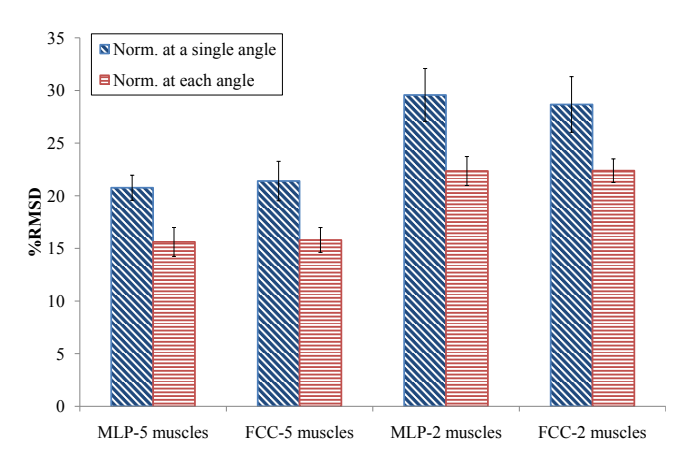


Figure 9. Mean lowest inter-day %RMSD for each normalization method and NN algorithm for the 10 days

approximately 40% (MLP, norm. to each angle) over using just two muscles. This result supports the opinion that, as different muscles contribute to the resultant torque with varying degrees, incorporating information from more muscles improves NN-based joint-torque estimation. Furthermore, neglecting sEMG data from principle knee extensors and flexors will compromise the ability of the NN to uniquely map sEMG-to-joint torque. The effect of incorporating data from more muscles when estimating day-to-day variations was also studied. The mean estimation errors achieved using the 8 best NN each day, to estimate joint torque for the other 9 days without prior learning, are plotted side by side in Fig. 9. An improvement of up to 30% (MLP, norm. to each angle) is achieved when data from all five muscles are used to train the NNs.

4.2. Data normalization

The lowest joint-torque estimation errors for both normalization methods for the 10 day period are plotted alongside each another in Fig.

8. The lowest individual %RMSD is 6.415% on day 4, whereas the mean lowest estimation error is 10.461% (1.792), achieved using results from category 8 (Fig. 4). These results are compelling evidence that normalizing the data to the maximum at each joint angle, on average, has better estimation accuracy than data that are normalized to the maximum at a single angle. This improvement is due to the fact that whilst the absolute value of the sEMG at different sites and angles may vary, the curve of the normalized sEMG to normalized joint torque at each angle is highly similar. Both [20, 22] recognize this relationship in certain types of muscles. In estimating inter-day variation (Fig. 9), data normalized using the second method lowers estimation errors in all four pairs by up to 25% compared to that from the first method.

4.3. NN architecture and training algorithm

This work also sought to identify an efficient NN that will provide consistent results over the three-week period. A fundamental assumption made when utilizing NNs is that a particular combination of muscle activities and joint angles will result in only one possible set of resultant joint torques. If this assumption is flawed then it is impossible to achieve repeatability. The effect of the two different NNs on joint-torque estimation is evident in Fig. 8. The MLP NN, on average, has a slightly better joint-torque estimation regardless of the data normalization method. As a result of the improvements incorporated in the novel NBN algorithm, it was expected that FCC network would outperform the MLP network. but the results indicate otherwise. Thus, for this implementation, the FCC network together with the NBN algorithm does not show significant improvement over the classical three layer MLP network. Despite the fact that the NBN algorithm has shown impressive results in other applications, its suitability for sEMG-to-joint-torque mapping is not immediately evident and has to be investigated further. The ability of both NNs to estimate joint torque for other days without prior training is very similar (Fig. 9), where the best estimation error is approximately 15% for each algorithm (5 muscles, normalized at each angle). This is almost a 50% increase in the estimation error compared to Fig. 8, suggesting that it is not feasible to use a pre-trained NN to estimate joint torque for another day.

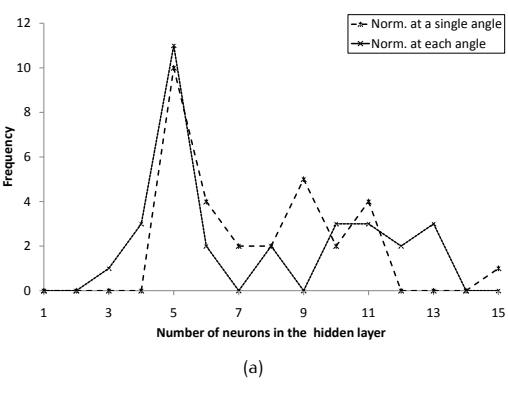
4.4. Neural network size

To ascertain the best network size to consistently produce near-optimal joint-torque estimation, each NN was trained repeatedly with an increasing number of neurons. The network sizes that produce the top three lowest estimates are plotted in Fig. 10 (only data from procedure B in Fig. 4 is used). The plot shows how often a particular network size results in the best $(1^{st}, 2^{nd} \text{ or } 3^{rd})$ isometric torque estimate. The network sizes that give consistent results for the FCC network are nine and ten, when normalized using the first and second method respectively. Five neurons in the hidden layer form the optimal size for the MLP network. Moreover, when compared to the FCC, the MLP has a more distinct optimal network size. In comparison, [13] proposes a MLP network with 15 neurons in the hidden layer (for isokinetic torque estimation). It is suggested that smaller networks have good interpolation abilities and can handle new patterns that have not been used when training the network [26]. This is evident in the MLP network where the optimum number of neurons in the hidden layer is just one less than the number of inputs to the network.

4.5. Isokinetic torque estimation

The maximum torque curve obtained for the isokinetic motion (Fig. 11) is consistent with known skeletal muscle characteristics, where the





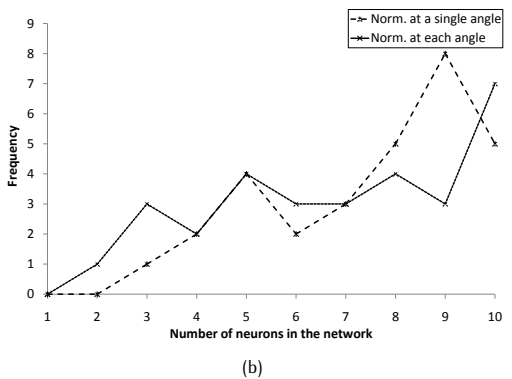


Figure 10. Frequency plot of optimal network sizes for MLP (a) and FCC (b) normalized using the frist method and second method

maximum torque exerted decreases with increasing joint velocity. Maximum concentric extensor torque occurred at ~50° knee angle whilst maximum concentric flexor torque occurred at ~25°. Each NN trained was tested with the normalized isokinetic data to determine the NN's ability to estimate dynamic torque. The principal assumption made in this estimation is that at low velocities, the motion of the knee joint could be approximated as a quasi-static movement, and isometric conditions may be presumed. Isokinetic torque estimation using NNs trained with isometric data yielded consistent results with a percentage error of about 20% to 30% (%RMSD). Over the 10-day period, the best isokinetic torque estimation achieved was 19.1349%. In Table 1, a typical isokinetic estimation result is shown. The mean estimation error at all velocities is very similar suggesting that the sEMG-to-joint-torque relation is similar for all the measured velocities and that quasi-static motion cannot be assumed at any velocity. The results show conclusively that NNs trained using isometric data alone cannot be used to reliably estimate isokinetic joint torque. One possible improvement may be to include known force-velocity relations and passive force characteristics as inputs to the NN. However, this finding does not conclusively prove that NNs trained using only isometric data cannot be used to estimate dynamic torque during activities of daily living ⁵. Isokinetic sEMG and torque were only used as an approximation and further tests need to be

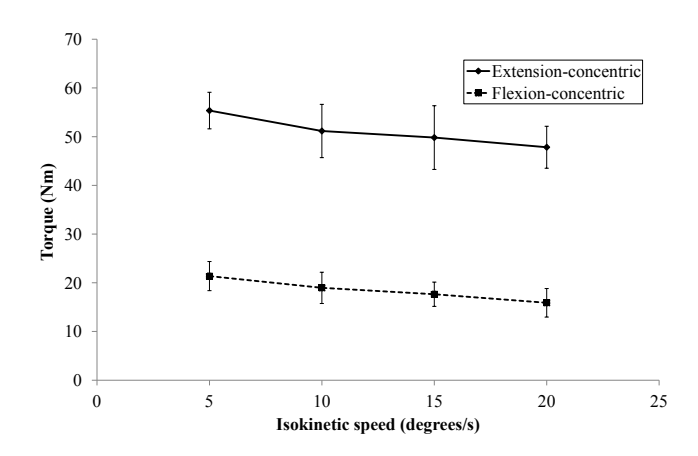


Figure 11. Mean maximum isokinetic torque

Speed	Test 1	Test 2	Test 3	Mean
$5^{o}s^{-1}$	30.3506	25.7914	24.1391	26.7604
$10^{o}s^{-1}$	34.1222	33.6545	22.1382	28.9716
$15^{o}s^{-1}$	32.1093	26.8430	24.4955	27.8159
$20^{o}s^{-1}$	21.9737	24.5017	30.9259	26.8004

Table 1. Typical results (%RMSD) for isokinetic torque estimation (MLP NN-5 neurons; 2nd normalization method)

conducted to determine the performance of the trained NNs for these activities.

Conclusion

The experiments carried out sought to investigate possible methods to improve NN based sEMG-to-torque estimation for the knee joint. Results indicate that including sEMG data from more extensor and flexor muscles significantly reduces estimation errors. This is because the contribution of the individual muscle groups to the resultant torque varies with the joint angle. Furthermore, data normalization at each isometric angle also improves estimation when compared to normalization at a single joint angle. The lowest estimation errors were achieved using NN trained with data from all five muscles that were normalized at each angle. When the best NNs from each day were used to estimate inter-day joint torque, the estimation error increases by approximately 50%. The comparison of the two NN shows that the FCC network is not a substantial improvement over the classical MLP. In addition, the MLP network is shown to have a better defined optimum network size (5 neurons) that produces consistent results. Experiments also revealed that estimating isokinetic torque from isometric data results in errors greater than 20% (%RMSD). One obvious limitation of the current work is that data were only gathered from one subject over three weeks. In order to further validate the effectiveness of the methodology, data should be gathered from more subjects over a similar time period.

 $^{^{\}rm 5}\,$ Walking, sit-to-stand movement, climbing and descending stairs, etc...

Acknowledgement

The authors would like to acknowledge the support of Festo AG & Co. KG, Mr. Campbell Lintott and Mr. Thomas Schönfelder.

References

- J. R. Cram, G. S. Kasman, and J. Holtz, Introduction to surface electromyography, 1st ed. Gaithersburg, Maryland: Aspen Publication, 1998
- [2] D. Staudenmann, K. Roeleveld, D. F. Stegeman, and J. H. van Dieen, Methodological aspects of semg recordings for force estimation-a tutorial and review, J. Electromyogr. Kinesiol., vol. 20, no. 3, (2010), 375–87
- [3] K. Lucas, The "all or none" contraction of the amphibian skeletal muscle fibre, The Journal of Physiology, vol. 38, no. 2-3, (1909), 113–33
- [4] J. V. Basmajian, Muscles alive. their functions revealed by electromyography, Journal of Medical Education, vol. 37, no. 8, (1962)
- [5] S. J. Day and M. Hulliger, Experimental simulation of cat electromyogram: evidence for algebraic summation of motor-unit action-potential trains, Journal of Neurophysiology, vol. 86, no. 5, (2001), 2144–58
- [6] K. G. Keenan and F. J. Valero-Cuevas, Epoch length to accurately estimate the amplitude of interference emg is likely the result of unavoidable amplitude cancellation, Biomedical Signal Processing and Control, vol. 3, no. 2, (2008), 154–162
- [7] C. J. De Luca, The use of surface electromyography in biomechanics, Journal of Applied Biomechanics, vol. 13, no. 2, (1997), 135–163
- [8] C. A. Doorenbosch and J. Harlaar, Accuracy of a practicable emg to force model for knee muscles, Neuroscience Letters, vol. 368, no. 1, (2004), 78–81
- [9] C. Fleischer, Controlling exoskeletons with emg signals and a biomechanical body model, Ph.D. dissertation, 2007
- [10] J.-J. Luh, G.-C. Chang, C.-K. Cheng, J.-S. Lai, and T.-S. Kuo, Isokinetic elbow joint torques estimation from surface emg and joint kinematic data: using an artificial neural network model, Journal of Electromyography and Kinesiology, vol. 9, no. 3, (1999), 173–183
- [11] S. Haykin, Neural networks and learning machines. Prentice Hall, 2009
- [12] M. M. Liu, W. Herzog, and H. H. C. M. Savelberg, Dynamic muscle force predictions from emg: an artificial neural network approach, Journal of Electromyography and Kinesiology, vol. 9, no. 6, (1999), 391–400
- [13] M. E. Hahn, Feasibility of estimating isokinetic knee torque using a neural network model, J. Biomech., vol. 40, no. 5, (2007),

1107-14

- [14] PhysioAdvisor.com, "Quadriceps and hamstring," 2011
- [15] D. Winter, Biomechanics and motor control of human movement, 4th ed. Wiley, 2009
- [16] H. J. Hermens and B. Freriks, SENIAM 5 The State of the Art on Sensors and Sensor Placement Procedures for Surface ElectroMyoGraphy: A proposal for sensor placement procedures, deliverable of the SENIAM project. Roessingh Research and Development b.v, 1999
- [17] C. J. De Luca and R. Merletti, Surface myoelectric signal cross-talk among muscles of the leg, Electroencephalography and Clinical Neurophysiology, vol. 69, no. 6, (1988), 568–575
- [18] C. J. De Luca, "Surface electromyography: Detection and recording," 2002
- [19] J. R. Potvin and S. H. M. Brown, Less is more: high pass filtering, to remove up to 99% of the surface emg signal power, improves emg-based biceps brachii muscle force estimates, Journal of Electromyography and Kinesiology, vol. 14, no. 3, (2004), 389–399
- [20] J. Perry and G. A. Bekey, Emg-force relationships in skeletal muscle, Crit. Rev. Biomed. Eng., vol. 7, no. 1, (1981), 1–22
- [21] J. R. Potvin, S. Brown, J. Dowling, and S. Tolmie, High pass filtering beyond 100 hz improves surface emg-based force predictions for the biceps brachii, Archives of Physiology and Biochemistry, vol. 108, no. 1-2, (2000), 156–156
- [22] C. Disselhorst-Klug, T. Schmitz-Rode, and G. Rau, "Surface electromyography and muscle force: Limits in semg-force relationship and new approaches for applications," Clinical Biomechanics, vol. 24, no. 3, (2009), 225–235
- [23] J. R. Potvin, R. W. Norman, and S. M. McGill, Mechanically corrected emg for the continuous estimation of erector spinae muscle loading during repetitive lifting, Eur. J. Appl. Physiol. Occup. Physiol., vol. 74, no. 1-2, (1996), 119–32
- [24] C. N. Maganaris, Force-length characteristics of in vivo human skeletal muscle, Acta Physiol. Scand., vol. 172, no. 4, (2001), 279–85
- [25] B. Wilamowski, Y. Hao, and C. Nicholas, NBN Algorithm, ser. Electrical Engineering Handbook. CRC Press, 2011, 1–24
- [26] B. M. Wilamowski, Neural network architectures and learning algorithms, Industrial Electronics Magazine, IEEE, vol. 3, no. 4, (2009), 56–63
- [27] B. M. Wilamowski, N. Cotton, J. Hewlett, and O. Kaynak, Neural network trainer with second order learning algorithms, in 11th International Conference on Intelligent Engineering Systems, 2007, 127–132
- [28] B. M. Wilamowski, N. J. Cotton, O. Kaynak, and G. Dundar, Method of computing gradient vector and jacobean matrix in arbitrarily connected neural networks, in IEEE International Symposium on Industrial Electronics, 2007, 3298–3303